Yi Lin and Zhongjie Sun

Antiaging Gene *Klotho* Attenuates Pancreatic β-Cell Apoptosis in Type 1 Diabetes

Diabetes 2015;64:4298–4311 | DOI: 10.2337/db15-0066

Apoptosis is the major cause of death of insulin-producing β-cells in type 1 diabetes mellitus (T1DM). *Klotho* is a recently discovered antiaging gene. We found that the *Klotho* gene is expressed in pancreatic β-cells. Interestingly, halplodeficiency of Klotho ($KL^{+/-}$) exacerbated streptozotocin (STZ)-induced diabetes (a model of T1DM), including hyperglycemia, glucose intolerance, diminished islet insulin storage, and increased apoptotic β-cells. Conversely, in vivo β-cell–specific expression of mouse *Klotho* gene (mKL) attenuated β-cell apoptosis and prevented STZ-induced diabetes. mKL promoted cell adhesion to collagen IV, increased FAK and Akt phosphorylation, and inhibited caspase 3 cleavage in cultured MIN6 β-cells. mKL abolished STZ- and TNFα-induced inhibition of FAK and Akt phosphorylation, caspase 3 cleavage, and β-cell apoptosis. These promoting effects of Klotho can be abolished by blocking integrin β1. Therefore, these cell-based studies indicated that Klotho protected β-cells by inhibiting β-cell apoptosis through activation of the integrin β1-FAK/Akt pathway, leading to inhibition of caspase 3 cleavage. In an autoimmune T1DM model (NOD), we showed that in vivo β-cell–specific expression of mKL improved glucose tolerance, attenuated β-cell apoptosis, enhanced insulin storage in β-cells, and increased plasma insulin levels. The beneficial effect of *Klotho* gene delivery is likely due to attenuation of T-cell infiltration in pancreatic islets in NOD mice. Overall, our results demonstrate for the first time that Klotho protected β-cells in T1DM via attenuating apoptosis.

Although type 1 diabetes mellitus (T1DM) affects 0.5% of the population in the developed countries (1), there is no cure for the devastating disease. The insulin replacement therapy remains the only choice for T1DM, which is susceptible to failure for appropriate control of blood glucose levels. T1DM results from immune-mediated destruction of the insulin-producing pancreatic β-cells (2). It has been estimated that at the time of diagnosis, patients with T1DM suffer from ~60–80% reduction in β-cell mass (3). It has been shown that β-cell apoptosis causes a gradual β-cell depletion in rodent models of T1DM (4). Both direct cytotoxic (T-cell mediated) and indirect cytokine-dependent (e.g., tumor necrosis factor-α) mechanisms are considered to be responsible for β-cell apoptosis (5). Thus, one of the goals in preventing T1DM is to preserve β-cells from apoptosis.

Klotho was identified as a putative aging-suppressor gene (6). In mice, overexpression of Klotho extended life span by 20–30%, whereas mutation of the *Klotho* gene caused numerous premature-aging phenotypes and shortened life span (7,8). The *Klotho* gene is primarily expressed in the kidneys and brain choroid plexus (7). Our most recent studies indicated that Klotho mRNA and proteins are also expressed in mouse pancreatic islets (9,10). In kidneys, the *Klotho* gene generated two types of transcripts, the full-length (130 kDa) and the short-form Klotho (65 kDa), due to alternative RNA splicing or proteolytic cleavage (6,11). We recently reported that only the short form of Klotho is expressed in pancreatic β-cells (9,10). Whether Klotho deficiency affects the development of T1DM is an interesting topic that was pursued in this study.

Multiple low doses of streptozotocin (STZ) have been shown to selectively destruct β-cells, which in turn induces immune reactions against pancreatic islets, leading to β-cell apoptosis and subsequently T1DM (12,13). This model resembles key features of human T1DM, including apoptosis and dysfunction of pancreatic β-cells. The STZ

Department of Physiology, College of Medicine, University of Oklahoma Health Sciences Center, Oklahoma City, OK

Corresponding author: Zhongjie Sun, zhongjie-sun@ouhsc.edu.

Received 14 January 2015 and accepted 25 August 2015.

This article contains Supplementary Data online at http://diabetes.diabetesjournals.org/lookup/suppl/doi:10.2337/db15-0066/-/DC1.

model demonstrates a loss of β-cell function and the development of hyperglycemia. Our recent study showed that Klotho attenuated β-cell damage in T2DM (10). T2DM is initiated by increased insulin resistance followed by hyperglycemia-induced β-cell damage. In contrast, the primary cause of T1DM is β-cell depletion. Thus, the major therapeutic strategy for T1DM is to protect β-cells. In this study, we investigated if in vivo expression of Klotho protects β-cell apoptosis and attenuates the development of T1DM induced by STZ.

Human T1DM is an autoimmune disorder that leads to the destruction of pancreatic β-cells. Therefore, we also investigated if *Klotho* gene delivery has beneficial effects in β-cells in nonobese diabetic (NOD) mice, an autoimmune model of T1DM. The NOD mouse is considered an autoimmune model of T1DM, which mimics the immunopathogenic features of human T1DM (14,15).

RESEARCH DESIGN AND METHODS

AAV Vector Construction and Recombinant Viral Production

The procedure for plasmid construction, viral package, and viral purification has been described in our recent study (10,16). In brief, β-cell–specific expression was achieved by AAV-2 delivery of the *Klotho* gene driven by a β-cell–specific promoter (rAAV-mKL) (10). Recombinant AAV-GFP (rAAV-GFP) was generated and used as a virus control (10).

Animal Studies in the STZ Model

This study was performed according to the National Institutes of Health Guide for the Care and Use of Laboratory Animals. This project was approved by the Institutional Animal Care and Use Committee at the University of Oklahoma Health Sciences Center. All mice were housed in cages at room temperatures 25 ± 1°C and were provided with Purina laboratory chow (no. 5001) and tap water ad libitum.

For *Klotho* gene deficiency study, we used heterozygous Klotho-deficient ($KL^{+/-}$) mice with more than nine generations in a 129Sv background, which were provided by Dr. M. Kuro-o (Department of Pathology, University of Texas Southwestern Medical School) (7,17). In brief, age-matched $KL^{+/-}$ and wild-type (WT) male mice (8–10 weeks) were injected with multiple low doses of STZ (50 μg/g/day, 5 days, i.p.) or citrate buffer, respectively. The WT littermate 129Sv mice were used as controls. STZ provokes β-cell destruction and immune reaction against pancreatic islets (12,13). Klotho homozygous ($Klotho^{-/-}$) mice demonstrate early and extensive aging phenotypes and die before the age of 8 weeks (body weight = 8 g) (7). Klotho homozygous mice also develop severe hyperphosphatemia and soft tissue calcification (6,18). As a result, Klotho homozygous mice were not used.

For the in vivo *Klotho* gene delivery study, male 129Sv mice were used (8 weeks, male) (The Jackson Laboratory, Bar Harbor, ME). In brief, PBS, rAAV-GFP, or rAAV-mKL was carefully injected, at the dose of 2.57×10^9 viral genome copies per gram body wt (500 μL), into the region of pancreas starting from the splenic lobes toward the duodenal lobes of pancreas via intraperitoneal delivery. One week later, these mice were injected with multiple low doses of STZ (50 μg/g/day, 5 days) or citrate buffer.

Body weight was monitored weekly. Blood glucose was measured weekly from the tail vein blood using a ReliOn Ultima glucose reader (Solartek Products, Inc., Alameda, CA). All mice were fasted for 3 h before glucose measurement.

Glucose Tolerance Test and Insulin Sensitivity Test

In experiments with $KL^{+/-}$ mice, the glucose tolerance test (GTT) was performed during weeks 2 and 4 after the initial injections of STZ. Insulin sensitivity test (IST) was performed during week 5 after the initial injections of STZ. In experiments with 129S1/SvIm mice, the GTT was performed during weeks 3 and 5 after the initial injections of rAAV. The IST was performed during week 6 after the initial injections of rAAV. In brief, blood glucose levels were measured at 30, 60, 90, and 120 min after subcutaneous injections of D-glucose (1 g/kg; Fisher Scientific) or insulin (1.0 units/kg; Sigma-Aldrich). The baseline glucose levels were determined before the injections of glucose or insulin after 3-h fasting.

Tissue Collections

The $KL^{+/-}$ mice were killed with an overdose of sodium pentobarbital (100 mg/kg, i.p.) at the end of week 5 after the initial injection of STZ. The 129S1/SvIm mice were euthanatized at the end of week 6 after rAAV delivery. For all mice, blood was collected before perfusion with heparinized saline. Plasma was stored at −80°C for later analysis of plasma insulin levels. Pancreas was fixed in 4% PBS-buffered paraformaldehyde for 24 h and then embedded in paraffin.

Animal Protocol for the NOD Model

Three groups of female NOD/ShiLtJ mice (stock 001976) and one group of female ICR/HaJ (stock 009122) mice were used (4 weeks; The Jackson Laboratory). Both NOD/ShiLtJ and ICR/HaJ mice are descended from ICR stock and carry the unique H2g7 MHC haplotype. However, ICR/HaJ mice do not develop diabetes and were used as controls. Blood glucose was measured weekly after 3-h fasting. At the beginning of the 14th week of age, three groups of NOD mice were treated with PBS, rAAV-GFP, and rAAV-mKL, respectively. The ICR/HaJ group was treated with PBS and served as controls. In brief, PBS, rAAV-GFP, or rAAV-mKL was carefully injected, at the dose of 2.57×10^9 viral genome copies per gram body wt (500 μL), into the region of pancreas starting from the splenic lobes toward the duodenal lobes of pancreas via intraperitoneal delivery (10). Glucose tolerance was tested at 7 and 14 days after gene delivery. Animals were killed at 16 days after gene delivery. Blood was collected for measuring plasma insulin levels. After perfusion with saline, pancreases were processed for fixation and paraffin embedding. The immunohistochemical staining

for Klotho, insulin, and/or T-cell infiltration was performed as described below.

Insulin Measurement

Plasma levels of insulin were measured using an insulin EIA kit according to the manufacturer's instructions (ALPCO Diagnostics, Salem, NH).

Immunohistochemistry

The immunohistochemistry (IHC) procedure was provided in our previous studies (10,11). In brief, these sections were incubated with antibodies against GFP (ab290; Abcam), Flag tag (ET-DY100; Aves Laboratories), CD3 (MCA1477; Bio-Rad), Klotho (R&D Systems), and insulin (sc-9168; Santa Cruz Biotechnology) overnight at 4°C and then with appropriated secondary antibodies conjugated with horseradish peroxidase at room temperature for 60 min. The islets of Langerhans in the cross sections of pancreas for each mouse were located under a microscope (Eclipse Ti; Nikon). Images of islets from consecutive cross sections for each animal were collected at equal exposure conditions and at the same magnification (40× objective lens). The staining density was quantified using ImageJ (NIH freeware) as mean gray value per pixel (10,11). The TUNEL assay on the cross sections of mouse pancreas was performed using TACS-XL Blue Label In Situ Apoptosis Detection Kit (Trevigen, Gaithersburg, MD). The number of cells with positive insulin or TUNEL staining in the islet was counted in NIS-Elements BR 3.0 (Nikon).

Cell Culture

Pancreatic insulinoma MIN6 β-cells were provided by Dr. Y. Miyazaki (Institute for Medical Genetics, Kumamoto University Medical School) and Dr. D. Steiner (Department of Biochemistry and Molecular Biology, University of Chicago) (19) and were cultured as described recently (10).

Transfection with Plasmid DNA

Plasmid DNAs including pAAV-CMV-mKL and pAAV-CMV-GFP were constructed as described previously (20) and purified with Qiagen Maxi Kit. For the MIN6 β-cell study, pAAV-CMV-GFP and pAAV-CMV-mKL were referred to as pGFP and pmKL, respectively. MIN6 β-cells cultured in six-well plates were transfected with various plasmid DNAs at the concentration of 0.072 μg/mL using Optifect reagent according to the manufacturer's protocol, followed by a 48-h incubation in DMEM with 10% FBS at 37°C in a 5% CO_2 incubator.

Cell Adhesion

Transfected cells (10^5 cells/well) were seeded on 48-well tissue culture plates coated with mouse collagen IV (5 μg/mL, catalog no. 35233; BD Biosciences) or 1% BSA and incubated in serum-free medium for 3 h. Nonadhered cells were removed and adhered cells were thoroughly washed. In brief, three to five random fields were imaged per well under a microscope (Eclipse Ti; Nikon). The number of cells that attached and spread were counted in NIS-Elements BR 3.0 (Nikon). For blocking experiments, transfected cells were preincubated with 5 μg/mL of integrin β1 blocking antibody (catalog no. ab24693; Abcam) or isoform control antibody IgG1 (catalog no. 401403; Biolegend) for 1 h before they were seeded on the plate.

Apoptosis Assay

Transfected cells were seeded on collagen IV–coated coverslips in a six-well plate and incubated in DMEM containing 10% FBS for 24 h. Cells were then in serum-free condition overnight before incubation with STZ (1 mmol/L), TNFα (40 ng/mL), IgG1 (5 μg/mL), or integrin β1 blocking antibody (5 μg/mL) for 24 h. Apoptotic nuclear changes were assessed with ApopTag Plus Peroxidase in Situ Apoptosis Detection Kit (Millipore). In brief, five random fields were imaged per well under a microscope (Eclipse Ti; Nikon). Apoptotic cells were assessed by nuclear staining color (brown) and condensation. The percentage of apoptotic cells was calculated for each field and averaged for the treatment group.

Western Blotting

In some experiments, cells were directly lysed in Ripa buffer containing protease inhibitor cocktail (catalog no. P8340, 1:100 dilution; Sigma-Aldrich) 48 h after the transfection. The lysates were directly subjected to SDS-PAGE followed by Western blotting with antibody against Klotho (AF1819; R&D Systems). The blot was rinsed and reprobed with antibody against β-actin as the loading control. In other experiments, transfected cells were seeded on collage IV–coated dishes and incubated in DMEM containing 10% BSA for 24 h. These cells were incubated in serum-free medium overnight and then treated with 1 mmol/L STZ, 40 ng/mL TNFα, IgG1 (5 μg/mL), or integrin β1 blocking antibody (5 μg/mL) for 24 h. Cells were lysed in Ripa buffer containing protease inhibitor cocktail (2.5 mmol/L sodium pyrophosphate, 1 mmol/L β-glycerolphosphate, 2 mmol/L sodium vanadate, 1 mmol/L EDTA, and 1 mmol/L EGTA). The protein concentration was measured with Pierce BCA assay (Thermo Scientific). Lysates (40 μg protein/well) under the reducing condition were directly subjected to SDS-PAGE (4–20% Tris-HCL precast gel; Bio-Rad) followed by Western blotting with antibody against p-Akt (Ser 473, catalog no. 4051; Cell Signaling Technology), p-FAK (Y397, catalog no. ab4803; Abcam), or cleaved caspase 3 (catalog no. 9664; Cell Signaling Technology), respectively. The same blot was reprobed with antibodies against Akt (catalog no. 4685; Cell Signaling Technology), FAK (catalog no. ab72140; Abcam), or caspase 3 (catalog no. 9662; Cell Signaling Technology) after stripping the blot, respectively. The same blot was stripped again and reprobed with antibody against β-actin as the loading control.

Immunoprecipitation

Transfected cells were lysed with Ripa buffer containing protease inhibitor cocktail. Lysates (500 μg/250 μL) were incubated with 1 μg integrin β1 antibody (catalog no. 610467; BD Biosciences) overnight at 4°C. Lysates were then incubated with 50 μL of 50% Protein A beads (catalog no. 16-125; Millipore) for 2 h. Immune complexes were pelleted and washed

with Ripa buffer five times. After the final wash, each pellet was resuspended in 100 μL of 2× Laemmli sample buffer containing β-mercaptoethanol and boiled for 5 min. Samples were subsequently analyzed through Western blotting.

Statistical Analysis

All data were expressed as mean ± SEM. Blood glucose was analyzed by a repeated-measures one-way ANOVA. The remaining data were analyzed by a one-way ANOVA. The Newman-Keuls procedure was used to reveal differences between groups. A probability value with $P < 0.05$ was considered to be statistically significant.

RESULTS

Haplodeficiency of Klotho ($KL^{+/-}$) Exacerbated the Development of T1DM Induced by STZ

To study the roles of endogenous Klotho in the development of T1DM, we used $KL^{+/-}$ and their littermate WT mice treated with multiple low doses of STZ (12,13). STZ caused hyperglycemia in both $KL^{+/-}$ and WT mice after 1-week treatment with STZ (Fig. 1*A*). Notably, $KL^{+/-}$ mice demonstrated more severe hyperglycemia than the WT mice (Fig. 1*A*), indicating that half deficiency of Klotho exacerbated T1DM in response to the STZ challenge.

To gain insights for the mechanism of Klotho action, we examined subcutaneous GTT at weeks 2 and 4 and subcutaneous IST at week 5 after the initial injection of STZ. Indeed, $KL^{+/-}$ and WT mice displayed glucose intolerance after STZ challenge. $KL^{+/-}$ mice demonstrated increased glucose intolerance versus the WT mice (Fig. 1*B–E*), suggesting that half deficiency of Klotho exacerbated β-cell damage in response to the STZ challenge. $KL^{+/-}$ and WT mice treated with STZ did not show a significant difference in IST (Fig. 1*F* and *G*). Thus, these data indicate that half deficiency of Klotho may directly impair pancreatic β-cell function rather than affect insulin sensitivity in STZ-induced diabetic mice.

In addition, the basal plasma insulin levels in $KL^{+/-}$ mice were significantly lower than those of WT mice (Fig. 1*H*). Both $KL^{+/-}$ and WT mice displayed lower plasma levels of insulin after the STZ challenge (Fig. 1*H*). $KL^{+/-}$ mice demonstrated lower insulin levels than WT mice after STZ treatments (Fig. 1*H*). Fasting urine glucose

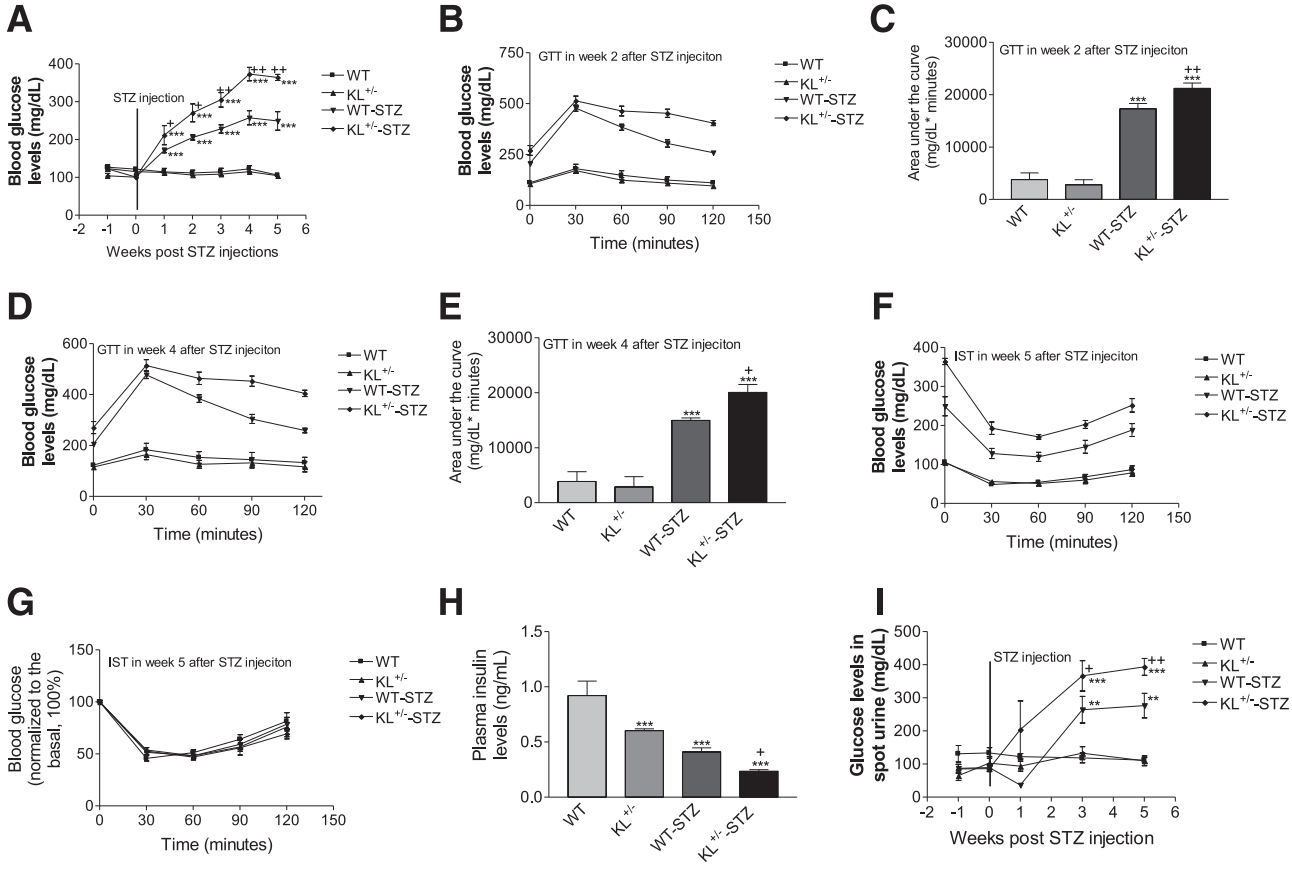

Figure 1—Half deficiency of Klotho in $KL^{+/-}$ mice exacerbated the development of T1DM induced by STZ. $KL^{+/-}$ and WT male mice were injected with STZ or citrate buffer. Blood glucose levels, glucose tolerance, insulin sensitivity, and plasma insulin levels were measured during the 5-week period. Fasting blood glucose levels (*A*). GTT results at week 2 (*B*) and week 4 (*D*) after the initial STZ injections. Area under the curve for GTT results at week 2 (*C*) and week 4 (*E*) after the initial STZ injections. Original readings of IST results at week 5 (*F*) after the initial STZ injections. Normalized blood glucose levels of IST results at week 5 (*G*) after the initial injections. Plasma insulin levels at week 5 after the injections (*H*). Urine glucose levels after the injections (*I*). Data = mean ± SEM. n = 4–8 animals/group. $^{**}P < 0.01$ and $^{***}P < 0.001$ vs. the WT group; $^{+}P < 0.05$ and $^{++}P < 0.01$ vs. the WT-STZ group.

levels were significantly higher in $KL^{+/-}$ mice versus WT mice treated with STZ (Fig. 1*I*). STZ decreased body weights in both WT and $KL^{+/-}$ mice (Supplementary Fig. 1*A*). However, the genotype difference did not alter body weight after the injection of STZ (Supplementary Fig. 1*A*). Therefore, endogenous Klotho deficiency exacerbated STZ-induced diabetes.

Haplodeficiency of Klotho ($KL^{+/-}$) Exacerbated STZ-Induced Cell Apoptosis and Depletion

IHC analysis indicated that Klotho staining in pancreatic islets of Langerhans was significantly lower in $KL^{+/-}$ mice versus WT mice (Fig. 2*A* and *B*). STZ did not alter Klotho staining.

There was no significant difference in insulin staining in pancreatic islets between the WT and $KL^{+/-}$ mice without STZ treatments (Fig. 2*C* and *D*). STZ decreased insulin staining in islets of WT and $KL^{+/-}$ mice. Interestingly, insulin staining was significantly lower in $KL^{+/-}$ mice than in WT mice after treatment with STZ (Fig. 2*C* and *D*). In addition, STZ caused a significant drop in the number of insulin-positive cells in pancreatic islets in both strains. STZ resulted in a greater drop in the number of insulin-positive cells in pancreatic islets in $KL^{+/-}$ mice than in WT mice (Fig. 2*C* and *E*). Therefore, Klotho deficiency predisposed mice to STZ-induced insulin depletion in pancreatic β-cells.

STZ caused an increase in the number of apoptotic cells in pancreatic islets in both strains (Fig. 2*F* and *G*). Notably, STZ led to a greater increase in the number of apoptotic cells in pancreatic islets in $KL^{+/-}$ mice versus WT mice (Fig. 2*F* and *G*). Therefore, half deficiency of Klotho predisposed pancreatic islet cells to STZ-induced apoptotic stimuli.

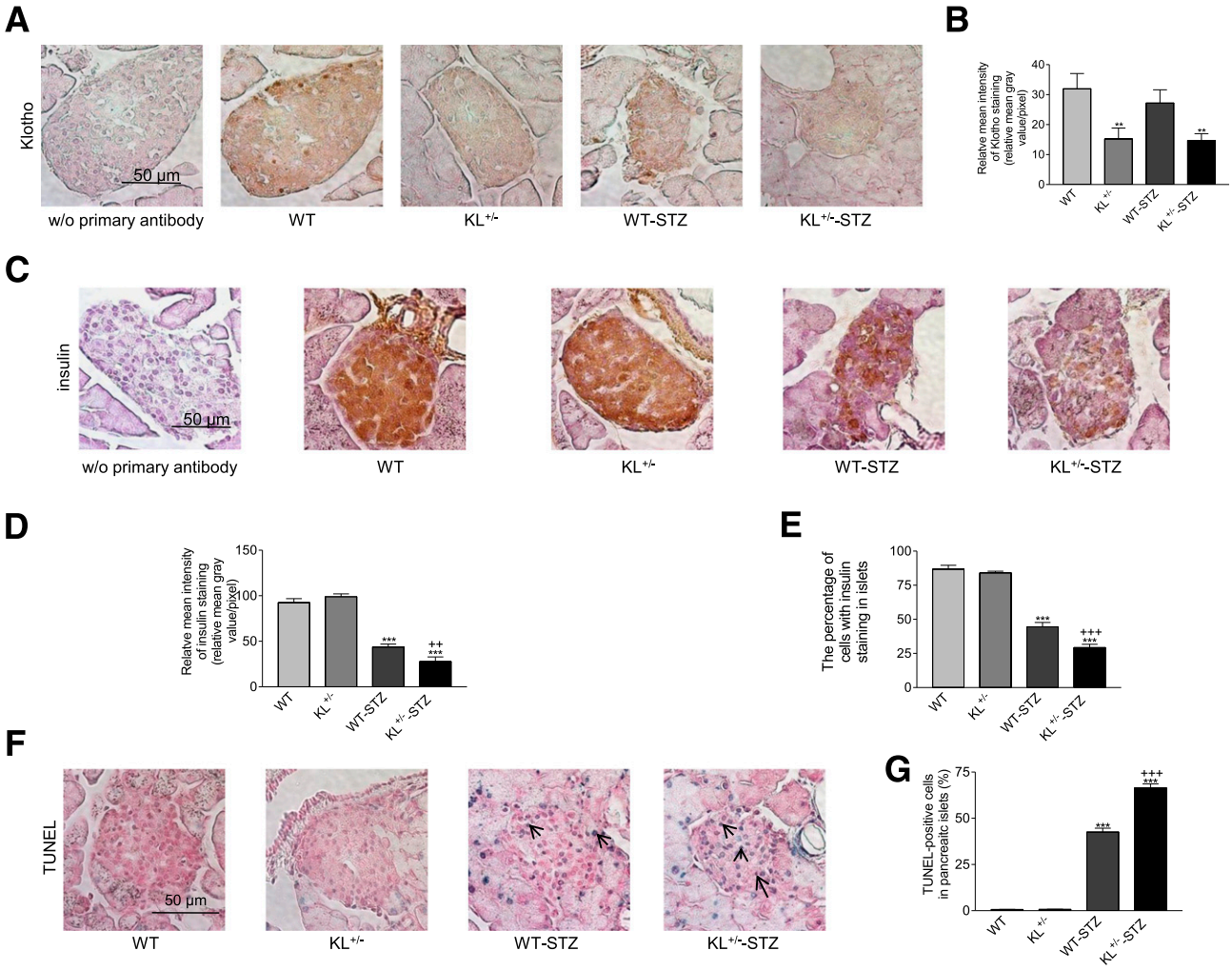

Figure 2—Immunohistochemical analysis of Klotho and insulin expression and apoptosis in pancreatic islets of mice treated with STZ. $KL^{+/-}$ and WT male mice were injected with STZ or citrate buffer. Animals were killed 5 weeks after the initial injections. *A*: Representative images of Klotho staining (brown color) in cross sections of mouse pancreatic islets. *B*: Semiquantification of Klotho staining in pancreatic islets. *C*: Representative images of insulin staining (brown color) of cross sections of islets. *D*: Semiquantification of insulin staining in pancreatic islets. *E*: The percentage of cells with positive insulin staining in pancreatic islets. *F*: Representative images of TUNEL staining (blue color) in pancreatic islets. Arrows point to apoptotic cells (blue). *G*: The number of TUNEL-positive apoptotic cells in pancreatic islets. Data = mean ± SEM. n = 4–8 animals/group. $^{**}P < 0.05$ and $^{***}P < 0.001$ vs. the WT group; $^{++}P < 0.01$ and $^{+++}P < 0.001$ vs. the WT-STZ group.

β-Cell–Specific Expression of mKL Attenuated the Development of Hyperglycemia in Mice Challenged with STZ

To test whether β-cell–specific expression of mKL attenuates hyperglycemia induced by STZ, we injected PBS, rAAV-GFP, or rAAV-mKL into 10-week-old male WT mice (129S1/SvIm) at the region of pancreas via intraperitoneal delivery. One week later, these mice were injected with multiple low doses of STZ or citrate buffer (control). As shown in Fig. 3*A*, injections of STZ caused mild hyperglycemia in these 129S1/SvIm mice. In contrast, rAAV-mKL prevented the development of hyperglycemia induced by STZ.

STZ caused glucose intolerance versus the control group (Fig. 3*B–E*). However, the treatment of rAAV-mKL prevented glucose intolerance compared with the PBS and rAAV-GFP–treated control groups (Fig. 3*B–E*). Injections of rAAV or STZ did not alter insulin sensitivity in 129S1/SvIm mice (Fig. 3*F* and *G*). Therefore, rAAV-mKL prevented STZ-induced hyperglycemia and improved glucose tolerance via preserving pancreatic β-cell function.

In addition, the STZ challenge caused a decrease in plasma insulin levels (Fig. 3*H*). In contrast, the treatments with rAAV-mKL attenuated the decrease in insulin levels (Fig. 3*H*), suggesting that rAAV-mKL may increase insulin release in 129S1/SvIm mice. No significant change in urine glucose was found in these mice (Fig. 3*I*). Injection of rAAV or STZ did not alter body weights in these 129S1/SvIm mice (Supplementary Fig. 1*B*). Therefore, β-cell–specific expression of mKL prevented hyperglycemia and glucose intolerance in STZ-treated animals.

β-Cell–Specific Expression of mKL Prevented Apoptosis in Pancreatic Islet Cells in STZ-Treated Mice

Several serotypes of rAAV have been used for pancreatic islet gene transfer with various efficiencies via different routes (21–23). In our rAAV construct, a Flag tag sequence was inserted at the 3′ end of mouse *Klotho* gene. Six weeks after the injections, we first examined GFP protein and FLAG tag in cross sections of paraffin-embedded pancreatic islets using IHC. Obviously, the intraperitoneal deliveries

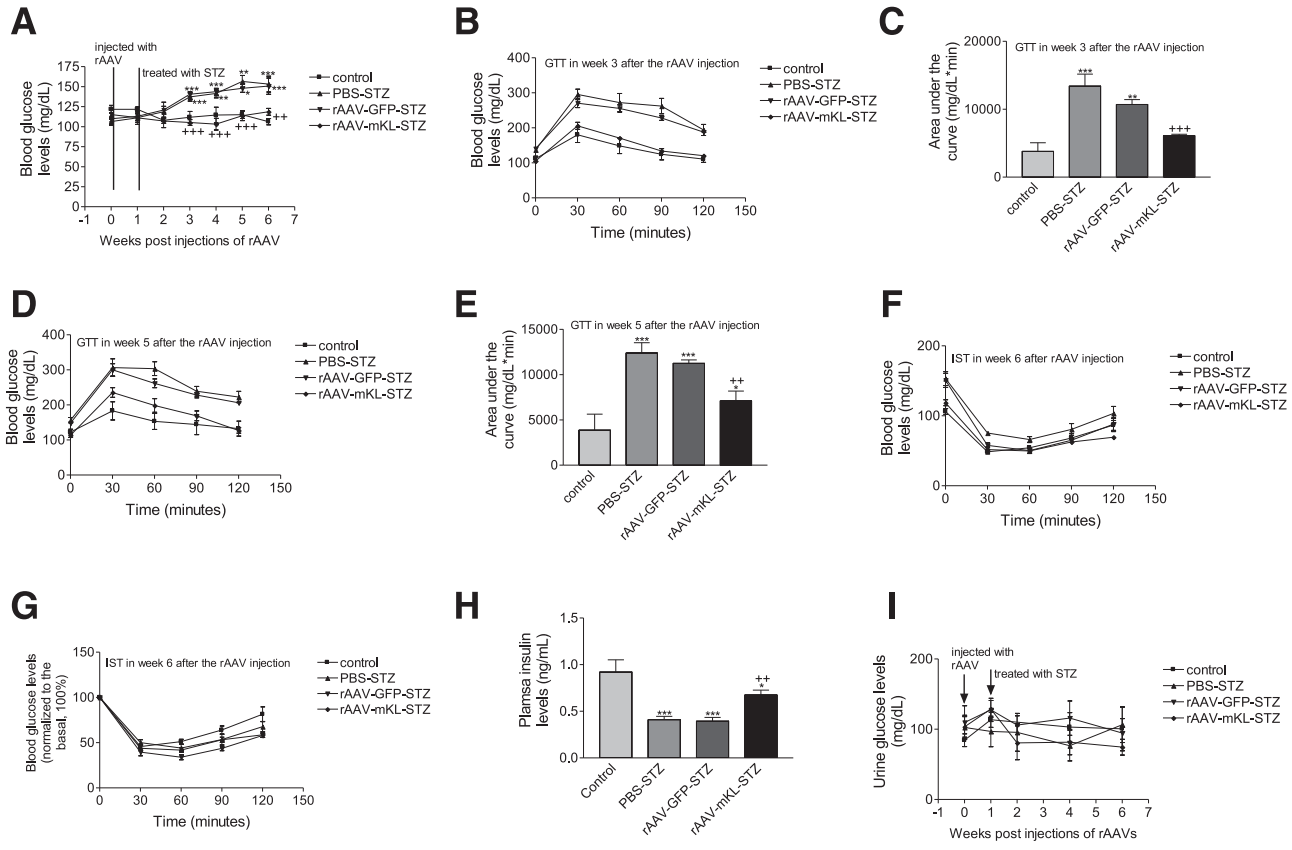

Figure 3—Effects of the β-cell–specific expression of mKL on blood glucose levels, glucose tolerance, insulin sensitivity, and plasma insulin levels in STZ-induced diabetic mice. 129S1/SvIm male mice were injected with PBS, rAAV-GFP, or rAAV-mKL, respectively. One week after gene delivery, these mice were injected with STZ or citrate buffer. Blood glucose levels, glucose tolerance, insulin sensitivity, and plasma insulin levels were measured during the 6-week period. Fasting blood glucose levels (*A*). GTT results at week 3 (*B*) and week 5 (*D*) after gene delivery. Area under the curve for GTT results at week 3 (*C*) and week 5 (*E*) after gene delivery. Original readings of IST results at week 6 (*F*) after gene delivery. Normalized blood glucose levels of IST results at week 6 (*G*) after gene delivery. Plasma insulin levels in mice at week 6 (*H*) after gene delivery. Urine glucose levels (*I*). Data are mean ± SEM. n = 4–6 animals/group. $^{*}P < 005$, $^{**}P < 0.01$, and $^{***}P < 0.001$ vs. the control (treated with PBS-citrate buffer) group; $^{++}P < 0.01$ and $^{+++}P < 0.001$ vs. the PBS-STZ–treated group.

of rAAV-GFP or rAAV-mKL drove GFP or FLAG tag expression in pancreatic islets of 129S1/SvIm mice (Supplementary Fig. 1*C* and *D*). These results confirmed that rAAV coupled with mouse insulin II promoter led to β-specific expression of target genes in mice.

The IHC analysis indicated that treatments with rAAV-mKL increased Klotho protein staining in pancreatic islets (Fig. 4*A* and *B*), suggesting effective gene delivery. In addition, STZ did not alter Klotho expression in pancreatic islets (Fig. 4*A* and *B*).

STZ decreased insulin staining and the number of β-cells in pancreatic islets (Fig. 4*C*–*E*). In contrast, β-cell–specific expression of mKL prevented the STZ-induced decreases in insulin staining (storage) and the number of β-cells in pancreatic islet (Fig. 4*C*–*E*). Therefore, β-cell–specific expression of mKL preserved pancreatic β-cell function and prevented the insulin depletion in pancreatic islets in STZ-treated mice.

STZ increased apoptosis in pancreatic islets of 129S1/SvIm mice (Fig. 4*F* and *G*). In contrast, β-cell–specific expression of mKL protected against STZ-induced apoptosis in pancreatic islets (Fig. 4*F* and *G*). Therefore, β-cell–specific expression of mKL prevented STZ-induced β-cell failure and apoptosis in pancreatic islets.

Expression of Klotho Attenuated Basal and STZ- and TNFα-Induced Apoptosis, Respectively, and Increased Cell Adhesion to Collagen IV in MIN6 β-Cells

We further studied the molecular mechanism underlying the beneficial effects of Klotho on β-cells using MIN6 β-cells. STZ and TNFα have been shown to cause apoptosis

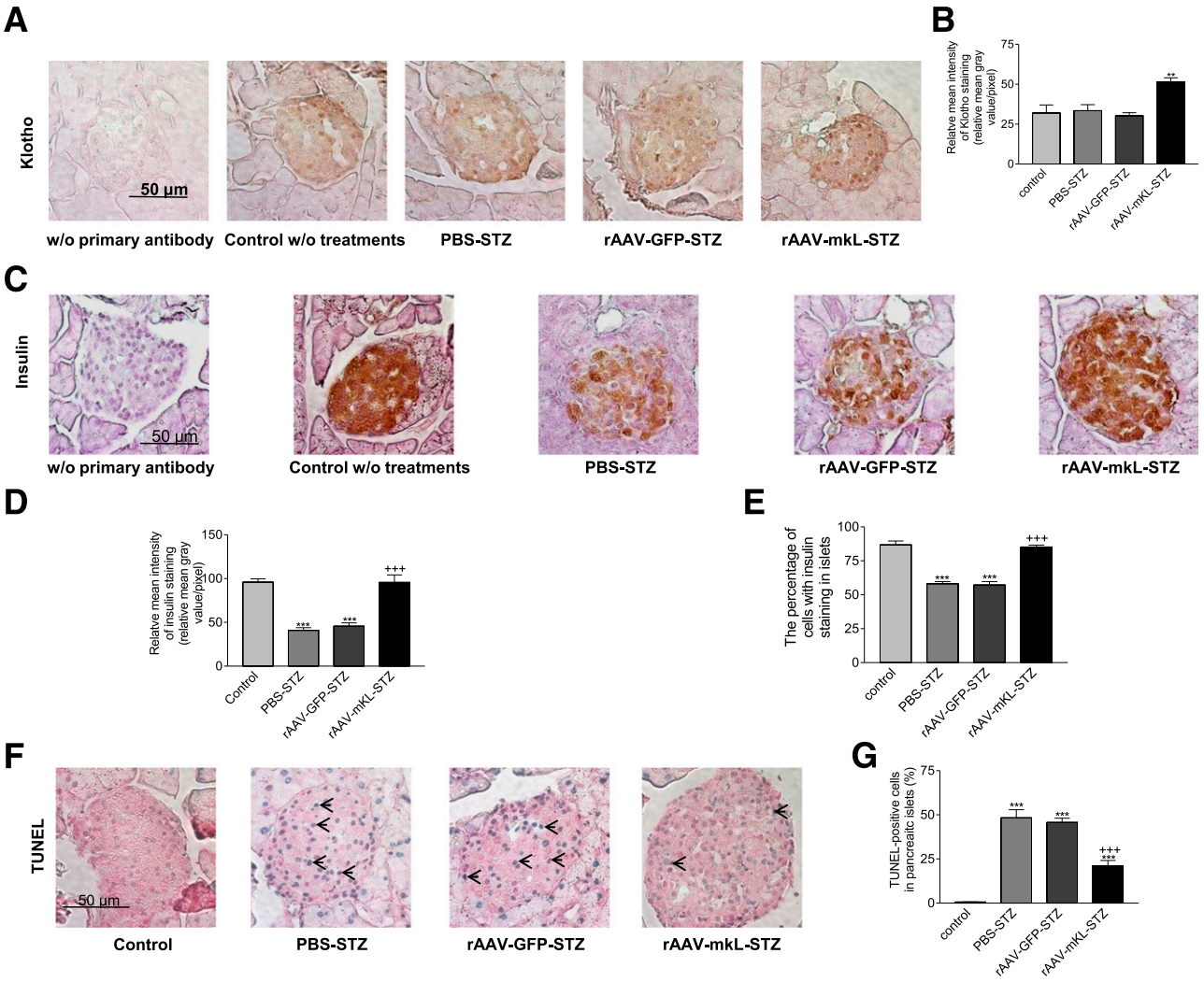

Figure 4—Effects of the β-cell–specific expression of mKL on insulin storage and apoptosis in pancreatic islets of mice challenged with STZ. 129S1/SvIm male mice were injected with PBS, rAAV-GFP, or rAAV-mKL. One week after gene delivery, these mice were injected with STZ or citrate buffer. Animals were killed 6 weeks after the rAAV injections. *A*: Representative images of Klotho staining (brown color) in cross sections of mouse pancreatic islets. *B*: Semiquantification of Klotho staining in pancreatic islets. *C*: Representative images of insulin staining (brown color) of cross sections of islets. *D*: Semiquantification of insulin staining in pancreatic islets. *E*: The percentage of cells with positive insulin staining in pancreatic islets. *F*: Representative images of TUNEL staining (blue color) in pancreatic islets. Arrows point to apoptotic cells. *G*: The number of TUNEL-positive apoptotic cells in pancreatic islets. Data = mean ± SEM. n = 4–6 animals/group. $^{**}P <$ 0.01 and $^{***}P <$ 0.001 vs. the control group; $^{+++}P <$ 0.001 vs. the PBS-STZ–treated group.

in MIN β-cells (24). Transfection of cells with plasmid DNA pmKL for 48 h increased Klotho protein in MIN6 β-cells (Fig. 5*A*–*C*). Interestingly, expression of mKL attenuated the basal, STZ-induced, and TNFα-induced apoptosis, respectively, in MIN6 β-cells as demonstrated by TUNEL staining (Fig. 5*D* and *E*). In addition, expression of mKL enhanced collagen IV–induced cell adhesion (Fig. 5*F* and *G*). Therefore, Klotho protected against apoptosis and promoted cell adhesion to collagen IV in MIN6 β-cells.

Expression of Klotho Promoted Phosphorylations of FAK and Akt and Decreased Caspase 3 Cleavage in MIN6 β-Cells

We found that expression of mKL increased phosphorylation of FAK and abolished the STZ-induced inhibition of phosphorylation of FAK in MIN6 β-cells (Fig. 6*A* and *B*). In addition, expression of mKL increased phosphorylation of Akt and abolished STZ-induced inhibition of phosphorylation of Akt in MIN6 β-cells (Fig. 6*C* and *D*). Furthermore, expression of mKL decreased caspase 3 cleavage and prevented STZ-induced caspase 3 cleavage in MIN6 β-cells (Fig. 6*E* and *F*). Therefore, the actions of Klotho involve upregulation of phosphorylation of FAK (an adhesion signaling) and phosphorylation of Akt (a survival signaling) as well as the inhibition of caspase 3 activity (a general apoptotic pathway). STZ suppressed expression of integrin β1, which can be abolished by expression of mKL (Fig. 6*G* and *H*). Thus, we will investigate if integrin β1 mediates the beneficial effect of Klotho.

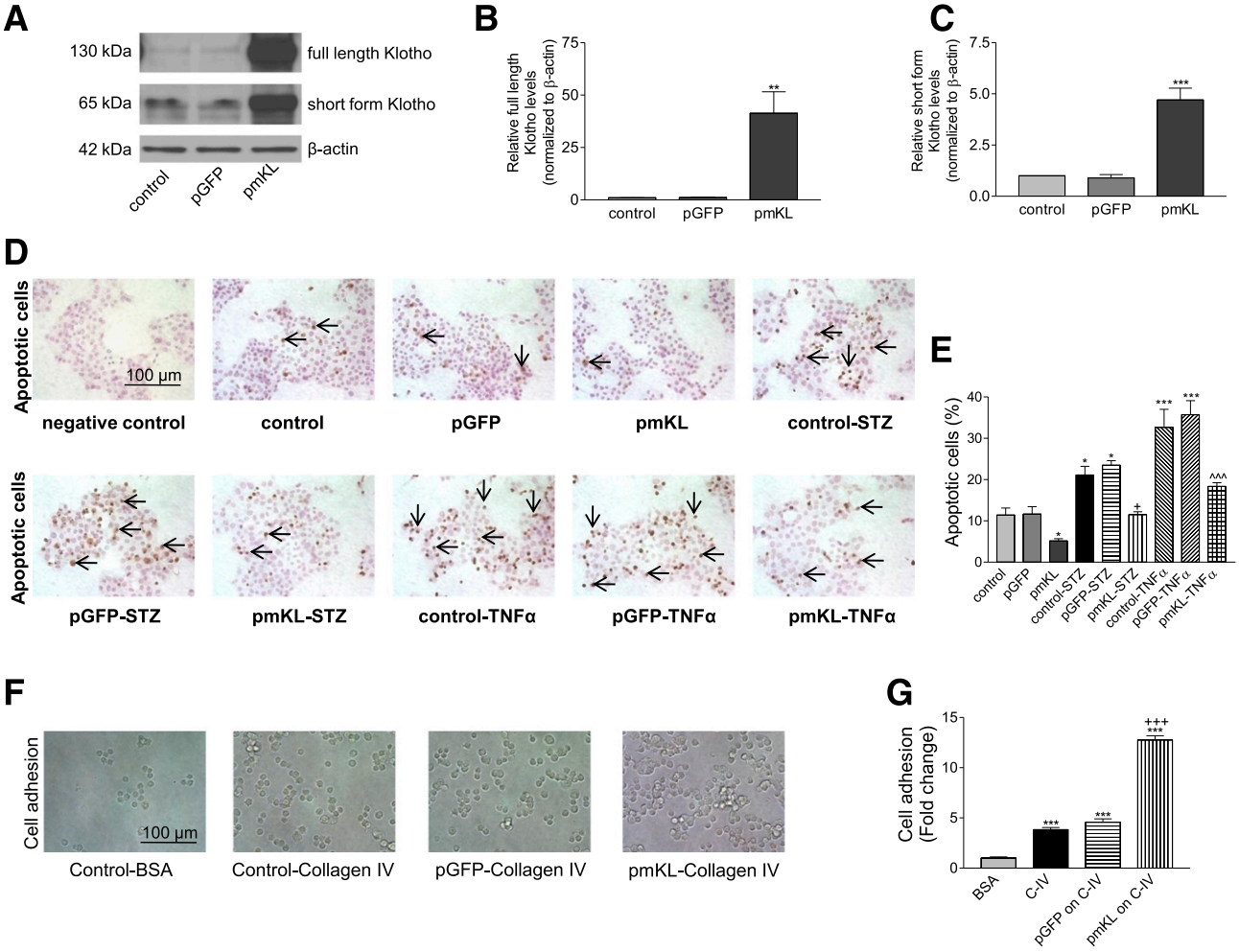

Figure 5—Effects of expression of mKL on basal and STZ-induced and TNFα-induced apoptosis, and cell adhesion to collagen IV in MIN6 β-cells. MIN6 β-cells were transfected with plasmid DNA including pmKL, pGFP, or vehicles (transfection agent alone) for 48 h. *A*: Western blot analysis of Klotho protein expression. *B*: Quantification of full-length Klotho protein expression. *C*: Quantification of short-form Klotho protein expression. Results were standardized to β-actin and then expressed as fold changes vs. the control group (transfection reagent alone). $n = 4$. $^{**}P < 0.01$ and $^{***}P < 0.001$ vs. the control group. *D*: Apoptotic nuclear change (pointed by arrows, brown color) detected by TUNEL staining in MIN6 β-cells. Transfected MIN6 β-cells were seeded on collagen IV–coated six-well plates and then incubated with or without STZ or TNFα for 24 h. *E*: The percentage of apoptotic cells. Data are means ± SEM. $n = 4$ wells. $^{*}P < 0.05$ and $^{***}P < 0.001$ vs. the control group; $^{+}P < 0.05$ vs. the control-STZ group; $^{\wedge\wedge\wedge}P < 0.001$ vs. the control-TNFα group. *F*: Phase contrast images of transfected MIN6 β-cells cultured in dishes coated with 1% BSA or collagen IV (5 μg/mL) for 3 h. *G*: Quantification of cell adhesion. $n = 4$ wells. $^{***}P < 0.001$ vs. the control-BSA group; $^{+++}P < 0.001$ vs. the control–collagen IV group.

Integrin β1 Was Required by Klotho for Protecting Against Apoptosis and Promoting Cell Adhesion

Next we investigated whether integrin β1 subunit, which acts as a receptor for extracellular matrix (ECM) including collagen IV with various integrin α subunits, was required for β-cell response to Klotho expression. Integrin β1 is expressed in mouse pancreatic islet cells and MIN6 cells (25). Blocking of integrin β1 using integrin β1 blocking antibody abolished the protection against apoptosis by Klotho in MIN6 cells (Supplementary Fig. 2*A* and *B*). In addition, blocking of integrin β1 attenuated Klotho-promoted cell adhesion to collagen IV (Supplementary Fig. 2*C* and *D*). Therefore, integrin β1 was required by Klotho for inhibiting apoptosis and promoting cell adhesion in MIN6 β-cells.

Integrin β1 Was Required by Klotho for Promoting Phosphorylation of FAK and Akt and Inhibiting Caspase 3 Cleavage

We found that blocking of integrin β1 attenuated the promoting effect of Klotho on phosphorylations of FAK and Akt in MIN6 cells (Supplementary Fig. 3*A* and *B*). Furthermore, blocking of integrin β1 abolished the inhibitory effect of Klotho on caspase 3 cleavage (Supplementary Fig. 3*C*). Thus, integrin β1 is required by Klotho for promoting phosphorylations of FAK and Akt and inhibiting caspase 3 cleavage. The coimmunoprecipitation assay revealed that Klotho was coimmunoprecipitated with integrin β1 (Supplementary Fig. 3*D*).

β-Cell–Specific Expression of mKL Abolished Glucose Intolerance and Increased Plasma Insulin Levels in NOD Mice

We further investigated the effect of in vivo β-cell–specific expression of Klotho in NOD mice, an autoimmune T1DM model. The NOD mice demonstrated glucose intolerance versus the control mice (ICR/HaJ) (Fig. 7*A*–*C*). Interestingly, rAAV-mKL abolished glucose intolerance in NOD mice. Plasma insulin levels were slightly but not significantly increased in NOD mice (Fig. 7*D*). Notably, rAAV-mKL significantly increased plasma insulin levels in NOD mice (Fig. 7*D*). Body weight was greater in NOD mice versus the control mice (Supplementary Fig. 4A). In vivo AAV delivery does not affect body weights in the three NOD groups. Blood glucose levels started to increase in NOD mice by 13 weeks of age (Supplementary Fig. 4*B*). rAAV-mKL attenuated the development of hyperglycemia and the percentage of patients with diabetes in NOD mice, although it did not reach a significant level (Supplementary Fig. 4*B* and *C*). The increase in blood glucose levels remained attenuated in NOD mice by rAAV-mKL after 16 days of gene delivery, although no statistical difference was found (Supplementary Fig. 4*D*).

β-Cell–Specific Expression of mKL Increased Insulin Storage and Attenuated T-Cell Infiltration and Apoptosis in Pancreatic Islets of NOD Mice

Klotho expression levels were decreased in pancreatic islets as evidenced by a decrease in Klotho staining (Fig. 8*A* and *B*). In vivo, β-cell–specific expression of mKL increased Klotho staining in NOD mice, suggesting effective gene delivery. Insulin was largely depleted in NOD mice (Fig. 8*C* and *D*). β-Cell–specific expression of mKL significantly increased insulin levels in NOD mice (Fig. 8*C* and *D*).

The number of CD3-positive T cells was increased in pancreatic islets in NOD mice (Fig. 8*E* and *F*). β-Cell–specific expression of mKL significantly decreased T-cell infiltration in NOD mice (Fig. 8*F*). The number of apoptotic cells was increased in islets in NOD mice, which can be attenuated by β-cell–specific expression of mKL (Fig. 8*G* and *H*).

DISCUSSION

This study demonstrated, for the first time, that haplodeficiency of Klotho in pancreatic islets predisposes mice to insulin-deficient diabetes induced by STZ. STZ-induced hyperglycemia, glucose intolerance, pancreatic islet apoptosis, and decreases in pancreatic insulin storage and plasma insulin levels were significantly exacerbated by deficiency of Klotho (Fig. 1). Most recently we found that knockdown of Klotho by siRNA significantly attenuated glucose-induced insulin secretion in MIN6 β-cells (9). Therefore, endogenous Klotho may be involved in the regulation of the physiological functions of β-cells. Notably, KL deficiency makes β-cells more susceptible to apoptotic stimuli (STZ) and predisposes to β-cell dysfunction (Figs. 1 and 2). Interestingly, β-cell–specific expression of Klotho preserved pancreatic β-cells from apoptosis, attenuated hyperglycemia, and enhanced the performance in glucose tolerance in STZ-treated mice (Figs. 3 and 4). Therefore, overexpression of Klotho in pancreatic β-cells is sufficient to preserve the physiological functions of β-cells in response to STZ challenge.

A key novel finding of the current study is that expression of mKL promoted cell adhesion to collagen IV, abolished STZ-induced inhibition of FAK and Akt, and attenuated STZ-induced caspase 3 cleavage and apoptosis in MIN6 β-cells (Figs. 5 and 6). Furthermore, we found that blocking of integrin β1 subunit abolished the promoting effects of Klotho on cell adhesion and phosphorylations of FAK and Akt as well as the protective effects of Klotho against apoptosis in MIN6 β-cells (Supplementary Figs. 2 and 3). Therefore, integrin β1 may contribute to the beneficial effects of Klotho in β-cells.

Several lines of evidence support our findings. The ECM stimulates a plethora of cellular processes, including cell differentiation, proliferation, survival, and function, by interacting with classical cell adhesion receptors, the integrins (26,27). Integrins are heterodimeric transmembrane molecules composed of distinct α and β subunits (28). Integrins have unique bidirectional signaling properties that incorporate the external and internal environments of a cell, allowing for dynamic coordination of extracellular events with intracellular changes (26). The major components of the ECM in pancreatic islets are collagen IV, laminins, and heparan sulfate proteoglycans such as perlecan

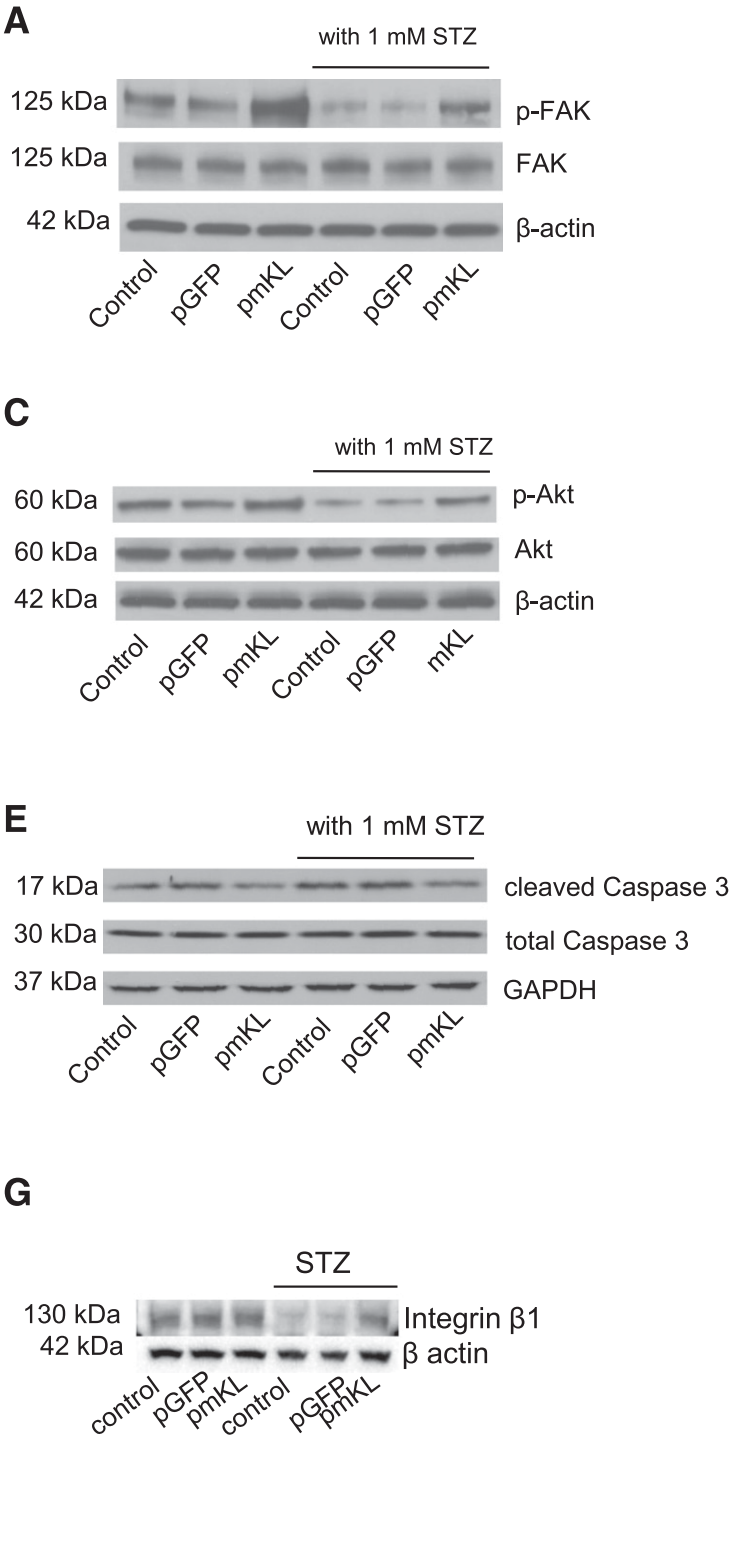

Figure 6—Expression of mKL increased phosphorylations of FAK and Akt and decreased caspase 3 cleavage in MIN6 β-cells. Transfected cells were seeded on collagen IV–coated six-well plates and then incubated with 1 mmol/L STZ for 24 h. Cells were lysed with Ripa buffer. *A*: Western blot analysis of phosphorylated FAK (Tyr 397; top panel) and FAK protein (middle panel) in cell lysates. *B*: Quantification of phosphorylation of FAK. Results were standardized to FAK protein levels and then expressed as fold changes vs. the control group. *C*: Western blot analysis of phosphorylated Akt (Ser 473; top panel) and Akt protein (bottom panel). *D*: Quantification of phosphorylation of Akt. Results were standardized to Akt protein levels and then expressed as fold changes vs. the control group. *E*: Western blot analysis of cleaved caspase 3 in cell lysates. *F*: Quantification of caspase 3 cleavage. Results were standardized to total caspase 3 and then expressed as fold changes vs. the control group. *G*: Western blot analysis of integrin β1. *H*: Quantification of integrin β1. $n = 4$ wells. $^{*}P < 0.05$, $^{**}P < 0.01$, and $^{***}P < 0.001$ vs. the control vehicle; $^{++}P < 0.01$ and $^{+++}P < 0.001$ vs. the control–1 mmol/L STZ group.

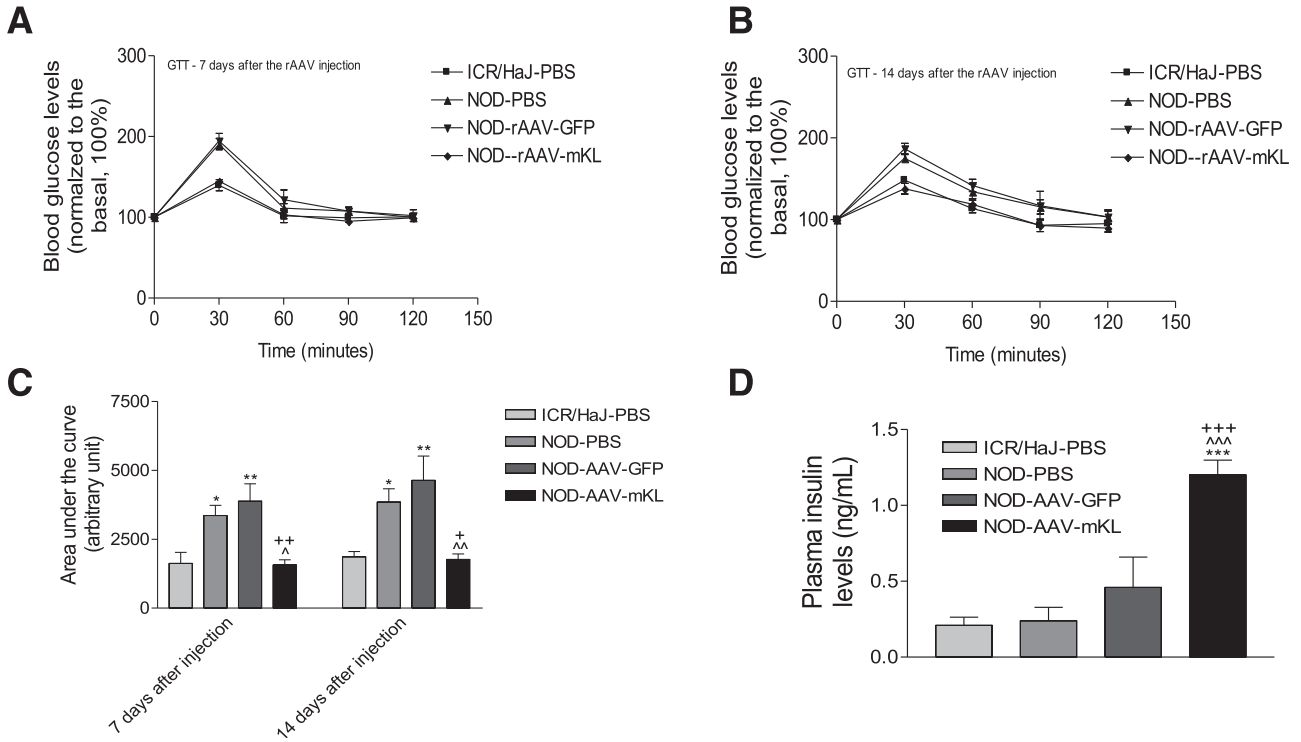

Figure 7—β-Cell–specific expression of mKL abolished glucose intolerance and increased plasma insulin levels in NOD mice. GTT was performed at 7 days (*A*) and 14 days (*B*) after gene delivery. Area under the curve for GTT results (*C*), ^^$P < 0.01$. Plasma insulin levels (*D*). Data are means ± SEM. $n = 5$ animals/group. *$P < 0.05$, **$P < 0.01$, and ***$P < 0.001$ vs. the ICR/HaJ-PBS group; ^$P < 0.05$ and ^^^$P < 0.001$ vs. the NOD-PBS group; $^{++}P < 0.01$ and $^{+++}P < 0.001$ vs. the NOD-AAV-GFP group.

(29). In isolated human islets, collagen IV has been shown to upregulate insulin secretion and β-cell survival (30,31). In vitro, collagen IV has been found to prevent MIN6 β-cells from apoptosis (32). In mouse pancreatic islets, heterodimers containing integrin β1 have been suggested to affect insulin transcription and secretion as well as β-cell proliferation (25). Integrin β1 has been shown to regulate rat β-cell (INS-1) survival (33). Male mice with a conditional knockout of integrin β1 in collagen I–producing cells display impaired glucose tolerance, with a significant reduction in pancreatic insulin contents and β-cell mass (34). In addition, FAK activation has been shown to be involved in glucose-stimulated insulin secretion in MIN6 β-cells, rat primary β-cells, or isolated islets (35,36). Most recent studies have shown that pancreatic β-cell–specific deletion of FAK attenuated β-cell viability and function in transgenic mice (37). Furthermore, Akt is believed to play important roles in the growth of β-cells and the protection of β-cells from apoptotic stimuli (38,39). Finally, caspase 3 knockout mice were protected from STZ-induced β-cell apoptosis and diabetes (12). Integrin β1 may be an important upstream mediator of Klotho-induced activation of FAK/Akt and inhibition of caspase 3 cleavage, which can be abolished by blocking of integrin β1 (Supplementary Fig. 3). Therefore, Klotho might protect β-cells from apoptosis and preserve β-cell function via interacting with integrin β1.

It has been reported that Klotho exhibited weak β-glucuronidase activity in vitro (40). Klotho participated in the removal of α2,6-linked sialic acids of TRPV5 through its sialidase activity in CHO cells (41). Removal of terminal sialic acids from *N*-glycans exposes underlying LacNAc for binding with galectin-1, leading to enhanced retention of TRPV5 at the cell surface (41). Based on the amino acid sequences, integrin β1 contains twelve potential asparagine-linked glycosylation sites, and desialylation of α5β1 integrin leads to increased adhesion to fibronectin, affecting cell adhesion in myeloid cells (42–44). Although Klotho can be coimmunoprecipitated with integrin β1 (Supplementary Fig. 3*D*), a further study is required for determining if Klotho physically interacts with integrin β1. On the other hand, Klotho activated the downstream signaling of integrin β1 (FAK/Akt-caspase 3) in MIN6 cells (Supplementary Fig. 3). Therefore, it would be interesting to investigate a hypothesis that Klotho targets sialic acid on the *N*-glycan of integrin β1 to regulate integrin signaling in MIN6 cells.

We note that haplodeficiency of Klotho decreased the basal plasma insulin level (Fig. 1*H*) but did not affect insulin storage levels in pancreatic islets (Fig. 2*C*–*E*). Therefore, KL deficiency may impair insulin release rather than insulin synthesis. This notion is supported by our recent study that Klotho enhances glucose-induced insulin release in MIN6 β-cells (9). Klotho promotes insulin release

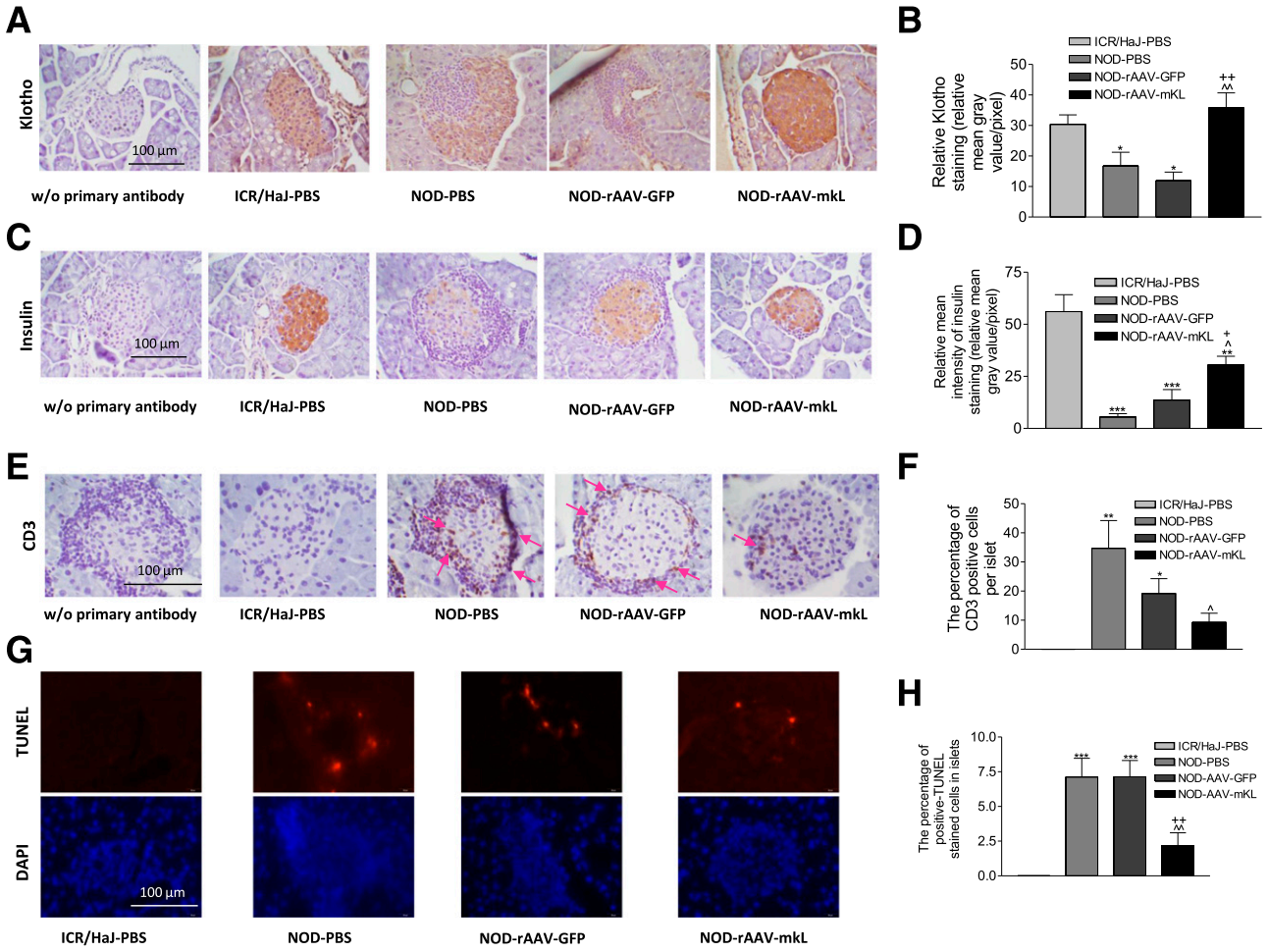

Figure 8—β-Cell–specific expression of mKL increased insulin storage and attenuated T-cell infiltration and apoptosis in pancreatic islets of NOD mice. *A*: Representative photomicrograph of Klotho staining (brown color) in cross sections of pancreatic islets. *B*: Semiquantification of Klotho staining in islets. *C*: Representative photomicrograph of insulin staining (brown color) in islets. *D*: Semiquantification of insulin staining in islets. *E*: Representative images of CD3 staining (brown color, red arrow) in islets. *F*: The percentage of cells with positive CD3 staining in islets. *G*: Representative images of apoptotic cells (TUNEL staining, immunofluorescence red color) in islets. *H*: The percentage of TUNEL-positive cells in islets. Data are mean ± SEM. $n = 5$ animals/group. $^{*}P < 0.05$, $^{**}P < 0.01$, and $^{***}P < 0.001$ vs. the ICR/HaJ-PBS group; $^{\wedge}P < 0.05$ and $^{\wedge\wedge}P < 0.01$ vs. the NOD-PBS group; $^{+}P < 0.05$ and $^{++}P < 0.01$ vs. the NOD–AAV-GFP group.

likely via increasing membrane retention of TRPV2 and intracellular levels of Ca^{2+} (9).

We also investigated the effects of β-cell–specific expression of Klotho in NOD mice, an autoimmune model of T1DM. NOD mice mimic the immunopathogenic features of human T1DM (14,15). The female NOD mice started to develop hyperglycemia spontaneously by 13 weeks of age (Supplementary Fig. 4*B*). We noticed that plasma insulin levels did not increase significantly (Fig. 7*D*) in the presence of hyperglycemia (Supplementary Fig. 4*B*) in NOD mice, which suggests a failure of β to respond to high blood glucose levels. The β-cell function was severely damaged in NOD mice as evidenced by impaired glucose tolerance (Fig. 7*A–C*). Interestingly, in vivo β-cell–specific expression of Klotho increased plasma levels of insulin (Fig. 7*D*) and abolished glucose intolerance in NOD mice (Fig. 7*A–C*). This study demonstrates, for the first time, that Klotho may also have therapeutic potential for autoimmune T1DM. Indeed, β-cell–specific expression of Klotho largely improved β-cell function, as evidenced by increased insulin storage levels in pancreatic islets in NOD mice (Fig. 8*C* and *D*).

β-Cells were damaged in NOD mice, as evidenced by the increased number of apoptotic β-cells (Fig. 8*G* and *H*), which is likely due to T-cell infiltration (Fig. 8*E* and *F*). Leukocyte infiltration is believed to be a major cause of β-cell damage in NOD mice (15,45,46). Interestingly, a decrease in Klotho in pancreatic islets was associated with T-cell infiltration (Fig. 8). The exciting and unique finding of this study is that in vivo β-cell–specific expression of Klotho attenuated T-cell infiltration and apoptotic damage to β-cells in NOD mice. Therefore, a decrease in Klotho may promote T-cell infiltration and β-cell apoptosis in NOD mice. We noticed that *Klotho* gene delivery did not decrease blood glucose to the control level (Supplementary Fig. 4*B–D*). This is probably due to the late treatment

with Klotho, which started at 14 weeks of age. Leukocyte infiltration into pancreatic islets occurred as early as 4 weeks of age in NOD mice (45). Thus, it is expected that an early intervention with *Klotho* gene delivery, e.g., before 4 weeks of age, may help achieve a better control of hyperglycemia in T1DM. In addition, we believe that a longer period of treatment with Klotho (e.g., 5 weeks) may further decrease blood glucose levels. A further study is warranted to explore how Klotho may attenuate leukocyte infiltration in NOD mice.

Klotho protected β-cells in T1DM and T2DM likely via different mechanisms. The beneficial effect of Klotho on β-cells in T2DM is mediated by suppression of oxidative stress and ER stress (10). Klotho protects β-cells in T1DM via the integrin pathway (STZ model) or suppression of T-cell infiltration in β-islets (NOD model).

In summary, Klotho deficiency promoted β-cell apoptosis in two models of T1DM. This study demonstrates, for the first time, that overexpression of Klotho effectively improved β-cell function and protected pancreatic β-cells in both STZ-treated mice and NOD mice. The beneficial effects of Klotho in β-cells are likely mediated via attenuating β-cell apoptosis. Hence, β-cell–specific expression of Klotho may find applications in the treatment of T1DM.

Funding. This work was supported by the National Institutes of Health (NIH) (DK093403, HL105302, HL102074, and HL118558). This publication was made possible by NIH grant 9P20GM104934-06 from the COBRE Program of the National Institute of General Medical Sciences.

Duality of Interest. No potential conflicts of interest relevant to this article were reported.

Author Contributions. Y.L. conducted the experiments, analyzed the data, and participated in writing the manuscript. Z.S. developed the concepts and hypotheses, designed the study, and participated in writing the manuscript. Z.S. is the guarantor of this work and, as such, had full access to all the data in the study and takes responsibility for the integrity of the data and the accuracy of the data analysis.

References

1. Mathis D, Vence L, Benoist C. Beta-cell death during progression to diabetes. Nature 2001;414:792–798
2. Rossini AA. Autoimmune diabetes and the circle of tolerance. Diabetes 2004;53:267–275
3. Notkins AL, Lernmark A. Autoimmune type 1 diabetes: resolved and unresolved issues. J Clin Invest 2001;108:1247–1252
4. Eizirik DL, Mandrup-Poulsen T. A choice of death–the signal-transduction of immune-mediated beta-cell apoptosis. Diabetologia 2001;44:2115–2133
5. Hui H, Dotta F, Di Mario U, Perfetti R. Role of caspases in the regulation of apoptotic pancreatic islet beta-cells death. J Cell Physiol 2004;200:177–200
6. Wang Y, Sun Z. Current understanding of klotho. Ageing Res Rev 2009;8:43–51
7. Kuro-o M, Matsumura Y, Aizawa H, et al. Mutation of the mouse klotho gene leads to a syndrome resembling ageing. Nature 1997;390:45–51
8. Kurosu H, Yamamoto M, Clark JD, et al. Suppression of aging in mice by the hormone Klotho. Science 2005;309:1829–1833
9. Lin Y, Sun Z. Antiaging gene Klotho enhances glucose-induced insulin secretion by up-regulating plasma membrane levels of TRPV2 in MIN6 β-cells. Endocrinology 2012;153:3029–3039
10. Lin Y, Sun Z. In vivo pancreatic β-cell-specific expression of antiaging gene Klotho: a novel approach for preserving β-cells in type 2 diabetes. Diabetes 2015;64:1444–1458
11. Zhou X, Chen K, Lei H, Sun Z. Klotho gene deficiency causes salt-sensitive hypertension via monocyte chemotactic protein-1/CC chemokine receptor 2-mediated inflammation. J Am Soc Nephrol 2015;26:121–132
12. Liadis N, Murakami K, Eweida M, et al. Caspase-3-dependent beta-cell apoptosis in the initiation of autoimmune diabetes mellitus. Mol Cell Biol 2005;25:3620–3629
13. Like AA, Rossini AA. Streptozotocin-induced pancreatic insulitis: new model of diabetes mellitus. Science 1976;193:415–417
14. Jayasimhan A, Mansour KP, Slattery RM. Advances in our understanding of the pathophysiology of type 1 diabetes: lessons from the NOD mouse. Clin Sci (Lond) 2014;126:1–18
15. Reed JC, Herold KC. Thinking bedside at the bench: the NOD mouse model of T1DM. Nat Rev Endocrinol 2015;11:308–314
16. Crosswhite P, Chen K, Sun Z. AAV delivery of tumor necrosis factor-α short hairpin RNA attenuates cold-induced pulmonary hypertension and pulmonary arterial remodeling. Hypertension 2014;64:1141–1150
17. Hsieh CC, Kuro-o M, Rosenblatt KP, Brobey R, Papaconstantinou J. The ASK1-signalosome regulates p38 MAPK activity in response to levels of endogenous oxidative stress in the Klotho mouse models of aging. Aging (Albany, NY) 2010;2:597–611
18. Xu Y, Sun Z. Molecular basis of Klotho: from gene to function in aging. Endocr Rev 2015;36:174–193
19. Miyazaki J, Araki K, Yamato E, et al. Establishment of a pancreatic beta cell line that retains glucose-inducible insulin secretion: special reference to expression of glucose transporter isoforms. Endocrinology 1990;127:126–132
20. Wang Y, Sun Z. Klotho gene delivery prevents the progression of spontaneous hypertension and renal damage. Hypertension 2009;54:810–817
21. Gaddy DF, Riedel MJ, Pejawar-Gaddy S, Kieffer TJ, Robbins PD. In vivo expression of HGF/NK1 and GLP-1 from dsAAV vectors enhances pancreatic β-cell proliferation and improves pathology in the db/db mouse model of diabetes. Diabetes 2010;59:3108–3116
22. Wang AY, Peng PD, Ehrhardt A, Storm TA, Kay MA. Comparison of adenoviral and adeno-associated viral vectors for pancreatic gene delivery in vivo. Hum Gene Ther 2004;15:405–413
23. Wang Z, Zhu T, Rehman KK, et al. Widespread and stable pancreatic gene transfer by adeno-associated virus vectors via different routes. Diabetes 2006;55:875–884
24. Zhang B, Lu Y, Campbell-Thompson M, et al. Alpha1-antitrypsin protects beta-cells from apoptosis. Diabetes 2007;56:1316–1323
25. Nikolova G, Jabs N, Konstantinova I, et al. The vascular basement membrane: a niche for insulin gene expression and beta cell proliferation. Dev Cell 2006;10:397–405
26. Kim SH, Turnbull J, Guimond S. Extracellular matrix and cell signalling: the dynamic cooperation of integrin, proteoglycan and growth factor receptor. J Endocrinol 2011;209:139–151
27. Reddig PJ, Juliano RL. Clinging to life: cell to matrix adhesion and cell survival. Cancer Metastasis Rev 2005;24:425–439
28. Berman AE, Kozlova NI, Morozevich GE. Integrins: structure and signaling. Biochemistry (Mosc) 2003;68:1284–1299
29. Kragl M, Lammert E. Basement membrane in pancreatic islet function. Adv Exp Med Biol 2010;654:217–234
30. Kaido T, Perez B, Yebra M, et al. Alphav-integrin utilization in human beta-cell adhesion, spreading, and motility. J Biol Chem 2004;279:17731–17737
31. Kaido T, Yebra M, Cirulli V, Montgomery AM. Regulation of human beta-cell adhesion, motility, and insulin secretion by collagen IV and its receptor alpha1beta1. J Biol Chem 2004;279:53762–53769
32. Weber LM, Hayda KN, Anseth KS. Cell-matrix interactions improve beta-cell survival and insulin secretion in three-dimensional culture. Tissue Eng Part A 2008;14:1959–1968

33. Krishnamurthy M, Li J, Fellows GF, Rosenberg L, Goodyer CG, Wang R. Integrin alpha3, but not beta1, regulates islet cell survival and function via PI3K/Akt signaling pathways. Endocrinology 2011;152:424–435
34. Riopel M, Krishnamurthy M, Li J, Liu S, Leask A, Wang R. Conditional β1-integrin-deficient mice display impaired pancreatic β cell function. J Pathol 2011; 224:45–55
35. Rondas D, Tomas A, Halban PA. Focal adhesion remodeling is crucial for glucose-stimulated insulin secretion and involves activation of focal adhesion kinase and paxillin. Diabetes 2011;60:1146–1157
36. Rondas D, Tomas A, Soto-Ribeiro M, Wehrle-Haller B, Halban PA. Novel mechanistic link between focal adhesion remodeling and glucose-stimulated insulin secretion. J Biol Chem 2012;287:2423–2436
37. Cai EP, Casimir M, Schroer SA, et al. In vivo role of focal adhesion kinase in regulating pancreatic β-cell mass and function through insulin signaling, actin dynamics, and granule trafficking. Diabetes 2012;61:1708–1718
38. Wang Q, Brubaker PL. Glucagon-like peptide-1 treatment delays the onset of diabetes in 8 week-old db/db mice. Diabetologia 2002;45:1263–1273
39. Wang Q, Li L, Xu E, Wong V, Rhodes C, Brubaker PL. Glucagon-like peptide-1 regulates proliferation and apoptosis via activation of protein kinase B in pancreatic INS-1 beta cells. Diabetologia 2004;47:478–487
40. Tohyama O, Imura A, Iwano A, et al. Klotho is a novel beta-glucuronidase capable of hydrolyzing steroid beta-glucuronides. J Biol Chem 2004;279:9777–9784
41. Cha SK, Ortega B, Kurosu H, Rosenblatt KP, Kuro-O M, Huang CL. Removal of sialic acid involving Klotho causes cell-surface retention of TRPV5 channel via binding to galectin-1. Proc Natl Acad Sci U S A 2008;105:9805–9810
42. Gu J, Taniguchi N. Regulation of integrin functions by N-glycans. Glycoconj J 2004;21:9–15
43. Seales EC, Shaikh FM, Woodard-Grice AV, et al. A protein kinase C/Ras/ERK signaling pathway activates myeloid fibronectin receptors by altering beta1 integrin sialylation. J Biol Chem 2005;280:37610–37615
44. Semel AC, Seales EC, Singhal A, Eklund EA, Colley KJ, Bellis SL. Hypo-sialylation of integrins stimulates the activity of myeloid fibronectin receptors. J Biol Chem 2002;277:32830–32836
45. Driver JP, Serreze DV, Chen YG. Mouse models for the study of autoimmune type 1 diabetes: a NOD to similarities and differences to human disease. Semin Immunopathol 2011;33:67–87
46. Chaparro RJ, Dilorenzo TP. An update on the use of NOD mice to study autoimmune (type 1) diabetes. Expert Rev Clin Immunol 2010;6:939–955